~~AIS-1009~~

N72-12094

Delta Modulation

Status Report

January 1, 1971 - July 1, 1971

Prepared for

National Aeronautics and Space Administration

Manned Spaceflight Center

Houston, Texas

under

NASA Grant NGR 33-013-063

CASE FILE COPY

Principal Investigator

Donald L. Schilling

Donald L. Schilling

Associate Professor

Department of Electrical Engineering

City College of New York

New York, New York 10031

Introduction

This status report summarizes several of the areas of research in the area of Delta Modulation being supported under NASA Grant NGR 33-013-063 during the period January 1, 1971 - July 1, 1971.

This research will be presented as a paper at the National Electronics Conference in October 1971. The Delta Modulation systems described here have been constructed and tested. A voice tape has been made to illustrate their operation at sampling frequencies of 19.2 kilobits/second (NASA quality) and 56 kilobits/second (Telephone quality).

Abstract

An optimum adaptive delta modulator-demodulator configuration is derived. This device utilizes two past samples to obtain a step size which minimizes the mean square error for a Markov gaussian source. The optimum system is compared using computer simulations with the linear delta modulator and an enhanced Abate delta modulator. In addition the performance is compared to the rate distortion bound for a Markov source. It is shown that the optimum delta modulator is neither quantization nor slope-overload limited.

The optimum system, an enhanced version of the Abate delta modulator and a linear delta modulator were tested and compared using sinusoidal, square-wave and pseudo-random binary sequence inputs. The results show that the output signal-to-noise ratio is independent of the input signal power and is subject only to the limitations of the hardware employed. In addition, voice was recorded using these systems. The demodulated voice indicates negligible degradation is caused by the optimum system and by the enhanced Abate system while the linear delta modulator suffers significant degradation at a sampling frequency of 56 kilobits/sec.

VARIABLE STEP-SIZE ROBUST DELTA MODULATION

Introduction

Delta modulation has received widespread attention recently due to the increased information rate possible, as compared to conventional source encoding schemes. However, the commonly studied linear delta modulator has severe limitations. The disadvantages and limited performance of the linear delta modulator has been described by O'Neal (1), Towozawa and Kaneko (2), Brolin and Brown (3), and Abate (4). The basic limitations are due to the narrow dynamic range produced by two inherent characteristics. The first is the granular or quantization noise produced by the finite step size of the system. The second is slope overload noise introduced when the system cannot follow the input signal. Hence, the delta modulator has only one optimum point; i.e. where the output signal to noise ratio is a maximum for a given input power. To overcome these basic problems, it is necessary to vary the step size of the system to cope with the changing input signal. Hence, an adaptive scheme.

Several different adaptive delta modulators, both continuous and discrete, have been presented in the recent past (2), (3), (4), (5). However, instead of obtaining an adaptive procedure empirically, as did the previous investigators, this paper presents an analytical approach to obtain an adaptive scheme which produces a least mean square error.

1. Digital Linear Delta Modulator

The encoder and decoder of a linear digital delta modulator are shown in Fig. 1. The input consists of samples of a continuous input waveform, normally a highly correlated sequence $\{s_k\}$. The difference between s_k and x_k, called d_k, is quantized into two levels to produce a sequence of positive and negative 1's denoted by $\{e_k\}$ The accumulator is used as a predictor, estimating the value of the next source sample. In the case of a noiseless channel, the decoder receives the sample e_k and then adds the estimate x_k from the accumulator to form an output sample r_k.

A digital computer simulation of the digital delta modulator with a first order Markov sequence having a Gaussian amplitude distribution as an input, results in the performance curve shown in Fig. 2. This curve has the same general shape as the performance curve of the continuous linear delta modulator. Note that the system is optimum for a very narrow range of input signal power, and the signal to noise ratio decreases on both sides of the optimum point. The slope for low input power is due to the granular noise produced by the finite step size fed to the accumulator. The downward slope for high input signal power is accounted for by the inability of the accumulator to follow the input. This condition is commonly called slope overload (1). In a practical application, these two detrimental factors severly limit the usefulness of the linear delta modulation scheme.

2. Digital Song Variable Step Size Delta Modulator

To minimize the granular noise that appears when the input signal amplitude is small, the quantizing step must also be small. However, to reduce the slope overload noise when the signal varies rapidly, the step size must increase and this increase must be fast enough so that the predictor will closely approximate the input signal. Fig. 3 shows the general structure of the variable step size delta modulation system.

In this delta modulation system, the same processor is used in both the encoder and decoder. The input sequence e^{k-1}, and the estimate sequence x^{k-1} are defined as

$$e^{k-1} = e_{k-1}, e_{k-2}, e_{k-3}, \cdots, e_1$$

and

$$x^{k-1} = x_{k-1}, x_{k-2}, x_{k-3}, \cdots, x_1$$

The processor operates on both sequences e^{k-1} and x^{k-1} to determine the optimum variable gain u_k.

The variable gain u_k multiplies e_k to obtain the appropriate step. By properly varying u_k, the granular noise and the slope overload noise are both decreased, and therefore, the dynamic range of the linear delta modulator is increased.

The following assumptions have been made so that a practical configuration for the optimum variable step-size delta modulator could be derived:

(1) The digital channel is error free.

(2) The input signal is generated by the following difference equation,

$$s_k = \rho_{k-1} s_{k-1} + \lambda_{k-1} \tag{1}$$

where λ_{k-1} is normal, zero mean, and has standard deviation $\sigma_{\lambda_{k-1}}$ Eq. (1) describes a first order Markov, Gaussian amplitude distributed signal, which is a reasonable model for many communication sources.

Referring to Fig. 3, the equation describing the encoder is seen to be,

$$x_k = x_{k-1} + u_{k-1} \operatorname{sgn}(s_{k-1} - x_{k-1}) \tag{2}$$

$$= x_{k-1} + u_{k-1} e_{k-1}$$

and the output equation is simply,

$$r_k = x_{k+1} \tag{3}$$

To obtain the optimum gain u_k, one minimizes the mean square error between input and output sample; i.e.

$$\min_{u_{k-1}} E\left\{ s_k - r_k (x^k, e^k) \right\}^2$$

To do this let

$$\alpha \triangleq E\left\{ s_k - r_k (x^k, e^k) \right\}^2$$

$$= \int_{-\infty}^{\infty} \cdots \int_{-\infty}^{\infty} P(x^k, e^k)\, d(x^k, e^k) \int_{-\infty}^{\infty} (s_k - r_k)^2 P(s_k \mid x^k, e^k)\, ds_k$$

where $d(x^k, e^k) \triangleq d x^k\, d e^k$

Since the inner integral and $P(x^k, e^k)$ are non-negative, α is minimized by minimizing the inner integral. Hence, to find the optimum u_k, one differentiates the inner integral with respect to u_k and sets the result equal to zero:

$$\frac{\partial}{\partial u_{k-1}} \int_{-\infty}^{\infty} (s_k - r_k)^2 P(s_k \mid x^k, e^k)\, d s_k = 0$$

$$u_k + x_k e_k - e_k \int_{-\infty}^{\infty} s_k P(s_k \mid x^k, e^k)\, d s_k = 0$$

Therefore,

$$u_k = e_k \left\{ E(s_k \mid x^k, e^k) - x_k \right\} \tag{4}$$

This result shows that the optimum step-size processor computes the conditional expectation of s_k given all past data(x^k and e^k), subtracts the past estimate x_k, and multiplies this result by the sign information, e_k.

The new estimate x_{k+1} can be found by substituting Eq. (4) into Eq. (2):

$$x_{k+1} = x_k + e_k^2 \left\{ E\left(s_k \mid x^k, e^k\right) - x_k \right\}$$

$$= E\left\{ s_k \mid x^k, e^k \right\} \tag{5}$$

Eq. (5) suggests that the adaptive delta modulation system utilizing the structure of the linear delta modulator with a variable step-size is equivalent to optimum estimation using all past and present data in the feedback path as shown in Fig. 4.

3. One Past Sample Case

In this section the optimum estimator is evaluated for the case where only the most recent sample is available for processing. The estimator equation for this case becomes,

$$r_k = \int_{-\infty}^{\infty} s_k \, P\left(s_k \mid e_k, x_k\right) d\, s_k$$

The conditional probability density function $P\left(s_k \mid e_k, x_k\right)$ is shown in Appendix I to be,

$$P\left(s_k \mid e_k, x_k\right) = \begin{cases} \dfrac{P\left(s_k\right)}{q^1\left(x_k/\sigma_{s_k}\right)} & ; s_k > x_k,\ e_k = +1 \\ 0 & ; s_k < x_k,\ e_k = +1 \\ \dfrac{P\left(s_k\right)}{q\left(x_k/\sigma_{s_k}\right)} & ; s_k < x_k,\ e_k = -1 \\ 0 & ; s_k > x_k,\ e_k = -1 \end{cases} \tag{6}$$

where $q'(x)$ and $q(x)$ are defined as,

$$q'(x) \triangleq \text{erfc}(x) \triangleq \frac{1}{\sqrt{2\pi}} \int_x^\infty \exp\left(-\tfrac{1}{2} y^2\right) dy$$

$$q(x) \triangleq 1 - q'(x)$$

and σ_{s_k} = standard deviation of s_k

Therefore the estimator equation becomes

$$r_k = \begin{cases} \dfrac{\sigma_{s_k} \exp\left(-x^2 / 2\sigma_{s_k}^2\right)}{\sqrt{2\pi}\, q'\left(x_k/\sigma_{s_k}\right)} & ; \quad e_k = +1 \\ -\dfrac{\sigma_{s_k} \exp\left(-x^2/2\sigma_{s_k}^2\right)}{\sqrt{2\pi}\, q\left(x_k/\sigma_{s_k}\right)} & ; \quad e_k = -1 \end{cases} \tag{7}$$

The resulting optimum one sample observation delta modulation system can then be implemented as shown in Fig. 5. The function generator is defined by Eq. (7). Computer simulations of Fig. 5 with a stationary Gaussian Markov input were performed. The system performance is discussed in Section 5.

4. Two Past Sample Case

In the structure for the one sample observation described in the above section, the most recent sample amplitude and the sign of the coded output are the only pieces of information used in the processing. Since the source sequence is Markov, the correlation and the difference between adjacent samples give additional information to the estimator.

For a system employing the past two-sample observations, the estimator equation is,

$$r_k = \int_{-\infty}^{\infty} s_k \, P\left(s_k \mid x_{k-1}^k, e_{k-1}^k\right) d s_k$$

In Appendix II, r_k is shown to be;

$$r_k = \begin{cases} \dfrac{\int_{-\infty}^{x_{k-1}} \left[\rho_{k-1}\, q'(z_{k-1})\, s_{k-1} + \dfrac{\sigma_{\lambda_{k-1}}}{\sqrt{2\pi}} \exp\left(-\frac{1}{2} z^2_{k-1}\right) \right] P(s_{k-1})\, ds_{k-1}}{\int_{-\infty}^{x_{k-1}} q'(z_{k-1})\, P(s_{k-1})\, ds_{k-1}}; & e_{k-1}=-1,\ e_k=+1 \quad (8\text{-a}) \\ \dfrac{\int_{x_{k-1}}^{\infty} \left[\rho_{k-1}\, q'(z_{k-1})\, s_{k-1} + \dfrac{\sigma_{\lambda_{k-1}}}{\sqrt{2\pi}} \exp\left(-\frac{1}{2} z^2_{k-1}\right) \right] P(s_{k-1})\, ds_{k-1}}{\int_{x_{k-1}}^{\infty} q'(z_{k-1})\, P(s_{k-1})\, ds_{k-1}}; & e_{k-1}=+1,\ e_k=+1 \quad (8\text{-b}) \\ \dfrac{\int_{x_{k-1}}^{\infty} \left[\rho_{k-1}\, s_{k-1}\, q(z_{k-1}) - \dfrac{\sigma_{\lambda_{k-1}}}{\sqrt{2\pi}} \exp\left(-\frac{1}{2} z^2_{k-1}\right) \right] P(s_{k-1})\, ds_{k-1}}{\int_{x_{k-1}}^{\infty} q(z_{k-1})\, P(s_{k-1})\, ds_{k-1}}; & e_{k-1}=+1,\ e_k=-1 \quad (8\text{-c}) \\ \dfrac{\int_{-\infty}^{x_{k-1}} \left[\rho_{k-1}\, s_{k-1}\, q(z_{k-1}) - \dfrac{\sigma_{\lambda_{k-1}}}{\sqrt{2\pi}} \exp\left(-\frac{1}{2} z^2_{k-1}\right) \right] P(s_{k-1})\, ds_{k-1}}{\int_{-\infty}^{x_{k-1}} q(z_{k-1})\, P(s_{k-1})\, ds_{k-1}}; & e_{k-1}=-1,\ e_k=-1 \quad (8\text{-d}) \end{cases}$$

where $z_{k-1} = \dfrac{x_k - \rho_{k-1}\, s_{k-1}}{\sigma_{\lambda_{k-1}}}$

Equation (8) involves integrals with the random variable x_{k-1} in the limits. The functional relationship between the estimator r_k and the estimates x_k and x_{k-1} is not apparent by simply considering these integral relations. To simplify the results and make the results more useful the following approximations are made:

$$q'(x) \approx \begin{cases} \frac{1}{2} e^{-ax^2} & x > 0 \\ 1 - \frac{1}{2} e^{-ax^2} & x < 0 \end{cases} \qquad a = \tfrac{1}{2} \qquad (9)$$

For the case of highly correlated input samples, i.e., $\sigma^2_{s_{k-1}} >> \sigma^2_{\lambda_{k-1}}$, Appendix III shows that Eq. (8) can be approximately reduced to the following;

$$r_k = \begin{cases} \frac{2}{\sqrt{2\pi}}\sigma_{\lambda_{k-1}} + \left\{x_k - \frac{\sigma_{\lambda_{k-1}}}{\sqrt{2\pi}} \frac{\exp(-\frac{1}{2}y_k^2)}{q(y_k)}\right\}, & e_{k-1}=-1,\ e_k=+1 \quad (10\text{-a}) \\ \frac{2}{\sqrt{2\pi}}\sigma_{\lambda_{k-1}} + \left\{x_k + \frac{\sigma_{\lambda_{k-1}}}{\sqrt{2\pi}} \frac{\exp(-\frac{1}{2}y_k^2)}{q'(y_k)}\right\}, & e_{k-1}=+1,\ e_k=+1 \quad (10\text{-b}) \\ -\frac{2}{\sqrt{2\pi}}\sigma_{\lambda_{k-1}} + \left\{x_k + \frac{\sigma_{\lambda_{k-1}}}{\sqrt{2\pi}} \frac{\exp(-\frac{1}{2}y_k^2)}{q'(y_k)}\right\}, & e_{k-1}=+1,\ e_k=-1 \quad (10\text{-c}) \\ -\frac{2}{\sqrt{2\pi}}\sigma_{\lambda_{k-1}} + \left\{x_k - \frac{\sigma_{\lambda_{k-1}}}{\sqrt{2\pi}} \frac{\exp(-\frac{1}{2}y_k^2)}{q(y_k)}\right\}, & e_{k-1}=-1,\ e_k=-1 \quad (10\text{-d}) \end{cases}$$

where

$$y_k = \frac{\rho_{k-1}x_{k-1} - x_k}{\sigma_{\lambda_{k-1}}}$$

The first term in Eq. (10) is contributed by the uncorrelated portion of the signal, while the second term is contributed by both the two sample difference in the previous estimations and the uncorrelated portion of the signal.

5. Simulation Performance

In this section the performance of each system is observed through computer simulations. The signal power to mean square error ratio is employed as the performance criterion. Each system was simulated by operating on 1000 consecutive stationary first order Markov, Gaussian amplitude distributed samples.

Figure 6 shows the output signal-to-noise ratio versus input signal power curves for the one sample observation case. The curves are flat and independent of input signal power; i.e., the slope overload and granular noise regions are avoided. For an uncorrelated source ($\rho=0$) all the information needed for the estimation is contained in the present sample while for a correlated source all the samples are needed for an optimum (in mean square error sense) estimation. Hence, the output signal-to-noise ratio is highest for ρ (correlation coefficient) = 0, as shown in Fig. 6.

The performance of the approximated two past sample observation case is shown in Fig. 7. The results show that the

output signal-to-noise ratio is once again independent of input signal power. However, the signal-to-noise ratios are much higher than that of the one sample observation case. Also, the system performs better for a more highly correlated source. The performance of the linear delta modulation system with the Markov inputs is also shown in Fig. 7 for comparison.

The performance using three or more past samples increases the signal-to-noise level above that of the two past sample case. However, a study of the three past sample case yields extremely complicated estimator equations and the simplification to obtain a practical system implementation is not feasible. Furthermore, comparison of the performance of the two sample case to that of the rate distortion bound shows that not much more improvement can be gained by using three past samples.

The rate distortion bounds for a first order Markov, Gaussian source for ρ (correlation coefficient) = 0.95 and for $\rho = 0.9$ are derived in Appendix III. The bounds are plotted in Fig. 8. The comparison shows that the signal-to-noise ratio for the two past sample case is only 3.1dB less than the rate distortion bound for $\rho = 0.95$, and only 3.2dB less than the rate distortion bound for $\rho = 0.9$.

6. Experimental Results

The design of an efficient encoding system usually requires some knowledge of the statistics of the signal on which it is to be used. However, in pratical communication systems, statistics of real signals are seldom known a priori. The system structure derived in the previous sections is adaptive to the known statistics of the input signal.

For the case of the two past sample observation, the realizeable algorithm used to determine the parameter $\sigma_{\lambda_{k-1}}$, using the past two estimated samples x_k and x_{k-1}, is

$$\sigma_{\lambda_{k-1}} = | x_k - x_{k-1} | \tag{11}$$

A piecewise linear approximation of the function generator is used to describe Eq. (10). The complete structure of the adaptive delta modulator is shown in Fig. 9.

Referring to Fig. 9, one sees that s_k is converted to digital form using an eight bit A/D converter. After the processing, the decoder is converted back to analog form using an eight bit D/A converter. The encoder transmits a binary signal obtained from the sign bit.

The entire system was constructed using DTL integrated circuits. The data rate was set at 56 kilobits/second. The minimum quantization step was limited to 0.04 volts and the maximum voltage was limited to $\pm$ 5 volts.

The function generators g_1 and g_2 shown in Fig. 9, have the form shown in Fig. 10. The slopes α and β may be adjusted for different types of input signals.

A. Response to a Square Wave Input

The response of the system to a 500 Hz square wave input is shown in Fig. 11 for $\alpha = 1$, $\beta = 0.5$, $\alpha = 1$, $\beta = 0$; and the linear delta modulator. When $\alpha = 1$ and $\beta = 0$, the step size is seen to increase and decrease linearly, which is equivalent to an enhanced Abate adaptive scheme with 256 control switches. Note that this system has different steady state quantization steps, while for the case where $\alpha = 1$ and $\beta = 0.5$ the quantizing step always reduces to the minimum step in the steady state. The square wave responses show that the system performs best with $\alpha = 1$ and $\beta = 0.5$.

B. Response to Sinusoidal Inputs

The output signal-to-noise ratio versus the input signal power curves shown in Figs. 12a & b were measured for different input frequencies. The slopes of the curves in the small signal region are caused by the quantizing noise of the A/D and D/A converters. If the logic would be extended to ten bit words, the flat portion would be extended 12dB in the low-signal direction. Thus, the number of bits could be increased as desired to enable the system to operate at signal levels as small as desired. The upper limit of the input signal power is due to the $\pm$5v limitation of the A/D and D/A converters.

For sinusoidal inputs the resulting curves show that $\alpha = 1$ and $\beta = 0$ the system performs the best.

C. Response to Random Data Sequences

The oscillograms shown in Fig. 13a & b show the eye patterns of the system responses to random data sequences. The input was obtained by passing the output of the pseudo-random sequence generator through a low pass filter. Fig. 13a shows the eye pattern of the linear delta modulator while Fig 13b shows the eye pattern of the adaptive delta modulator with $\alpha = 1$ and $\beta = 0.5$. The results clearly show that the adaptive systems have much better ability in reconstructing the data.

D. Subjective Test of Speech Input

Subjective tests of speech to the adaptive ΔM was also performed. The adaptive scheme yielded orders of magnitude improvement in clarity over the linear delta modulator. Negligible degradation of speech was obtained using $\alpha = 1$ and $\beta = 0$ at 56 kilobits/second.

7. Conclusions

The general structure of the variable step size digital adaptive delta modulator was derived and proved to be equivalent to optimum estimation at the encoder and decoder. The special case of the two past sample observation was found to be comparatively simple to construct and useful for practical applications. The structure was derived by assuming known statistics of a first order Markov process. However, in the implemented system, the design included continuous estimation of the parameters of the input signal. Hence, the signal statistics were not needed a priori.

The system was designed and constructed for real time operation using all digital hardware and was tested for several deterministic signals as well as pseudo-random data sequences. The experimental results show that the system performance was quite good for all types of input signals. With extended hardware the output signal-to-noise ratio can be made relatively independent of the input signal power.

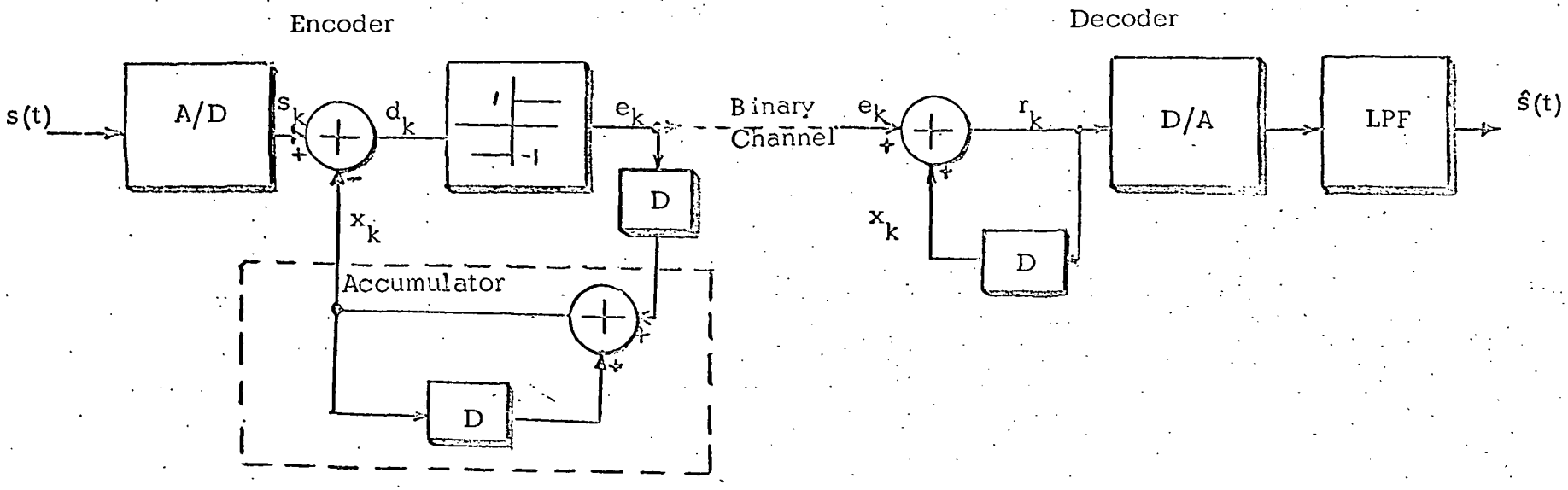

Fig. 1 Block Diagram of a Digital Linear Delta Modulator

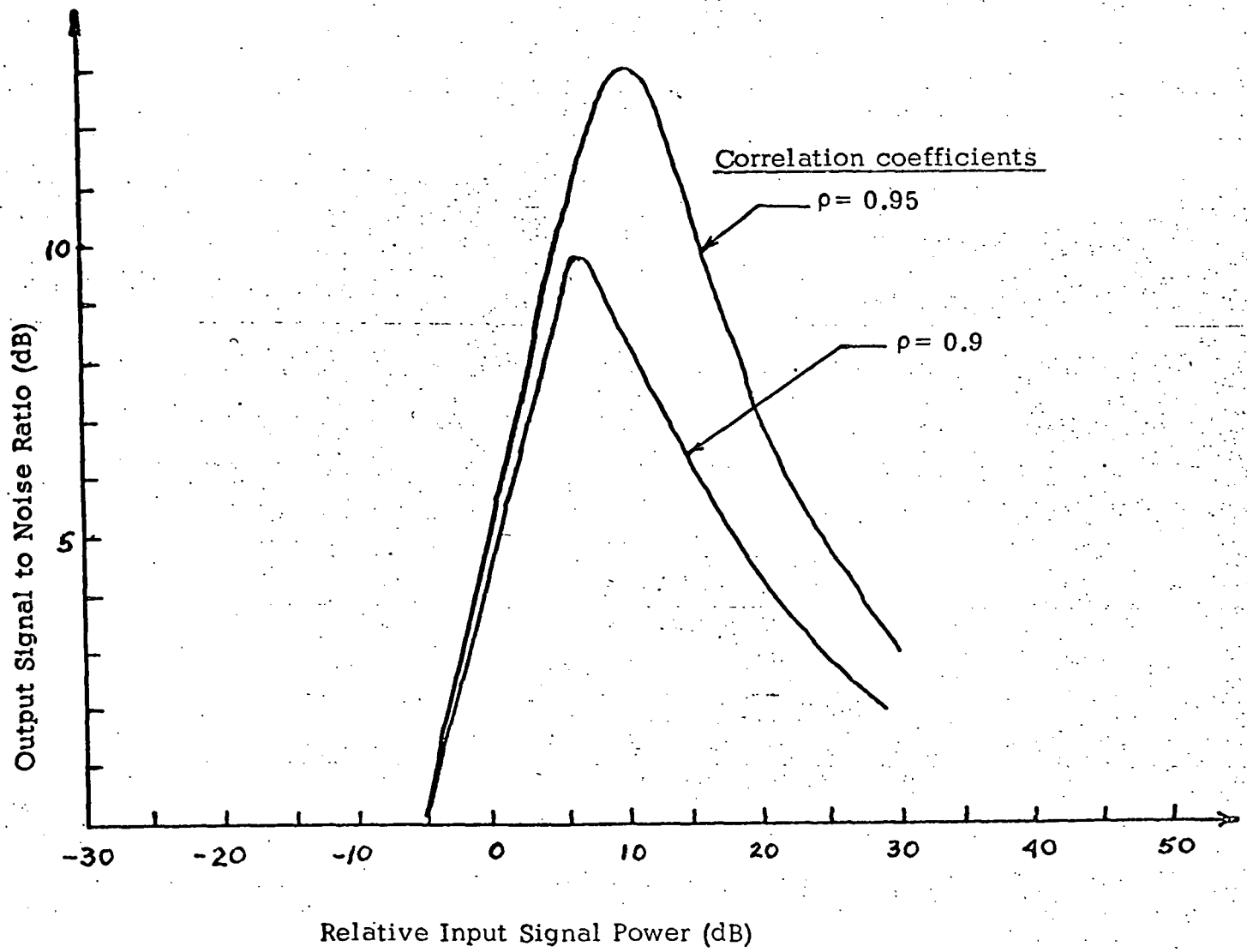

Fig. 2 Performance Curves of a Linear Digital Delta Modulator

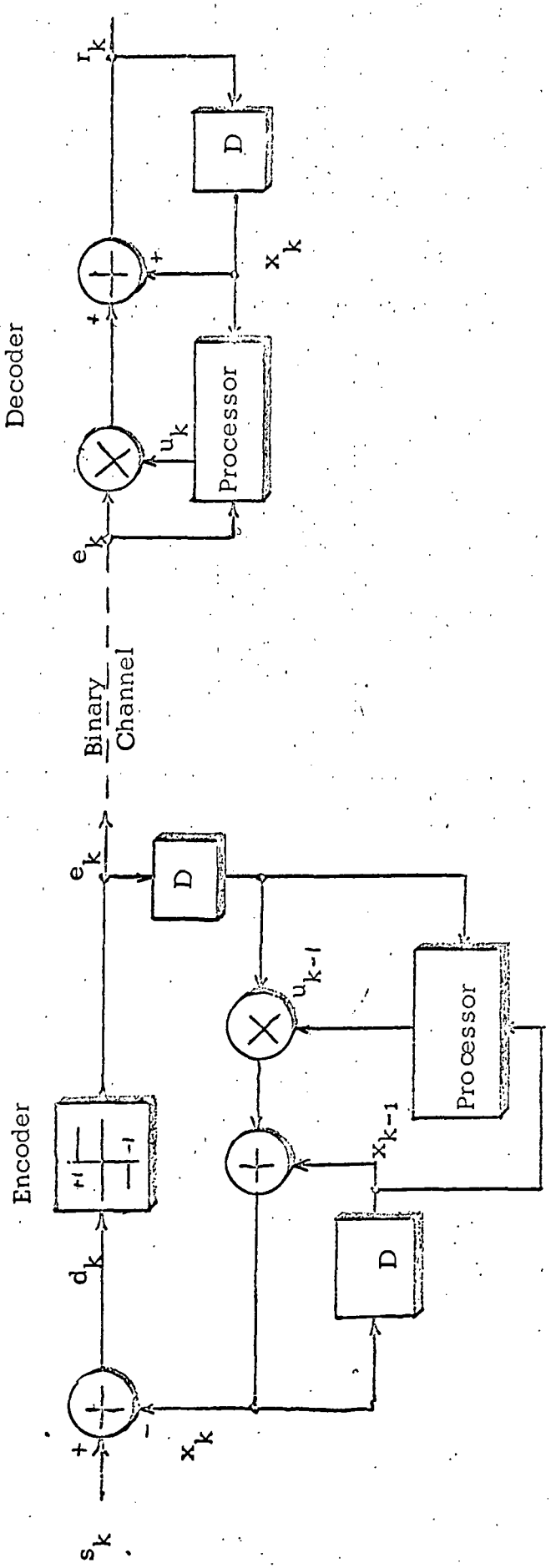

Fig. 3 Variable Step Size Adaptive Delta Modulation System

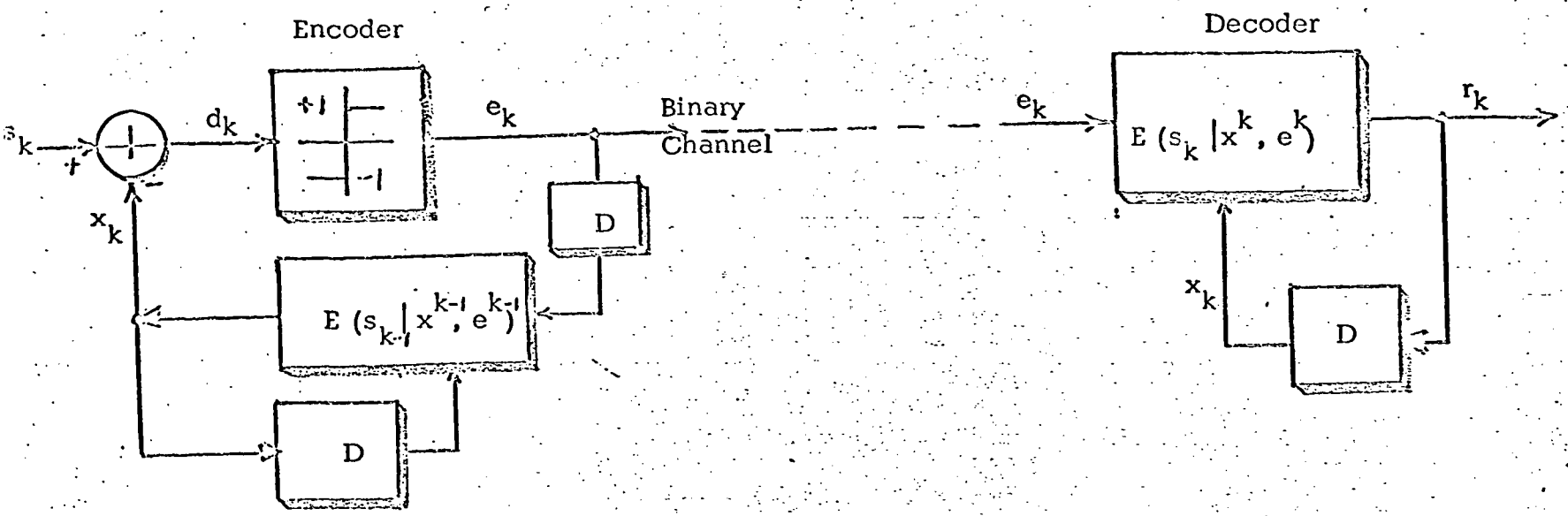

Fig. 4 Equivalent Optimum Step Size Adaptive Delta Modulation System

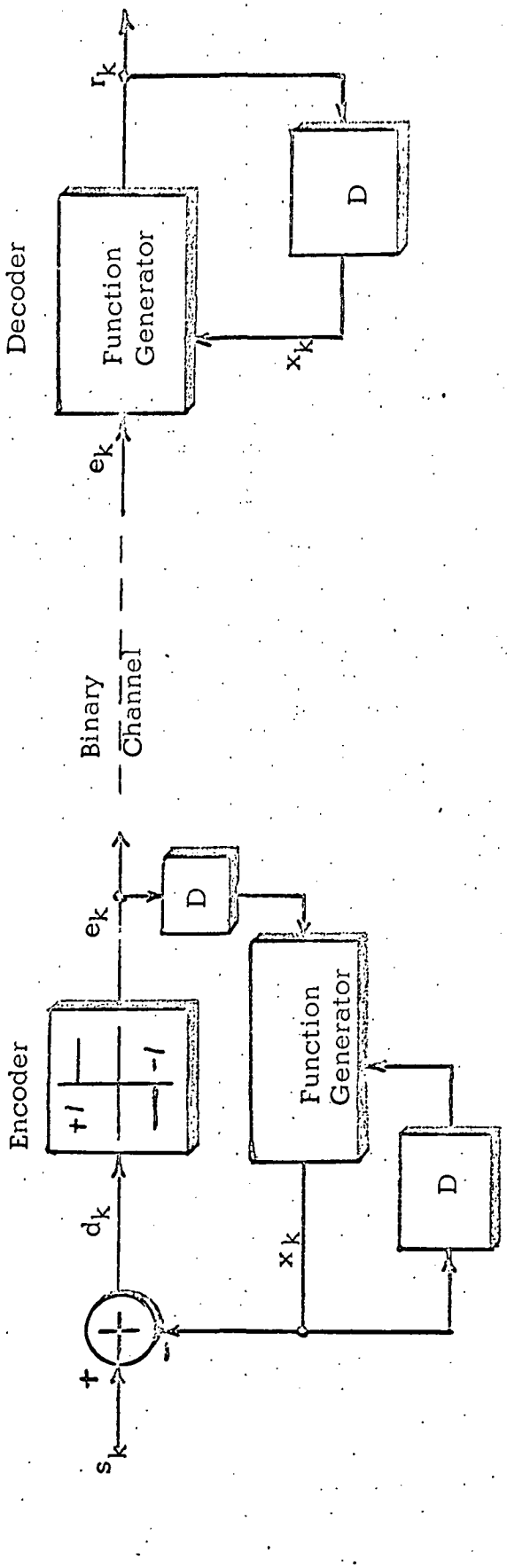

Fig. 5 Optimum Variable Step Size Delta Modulator One Past Sample Observation

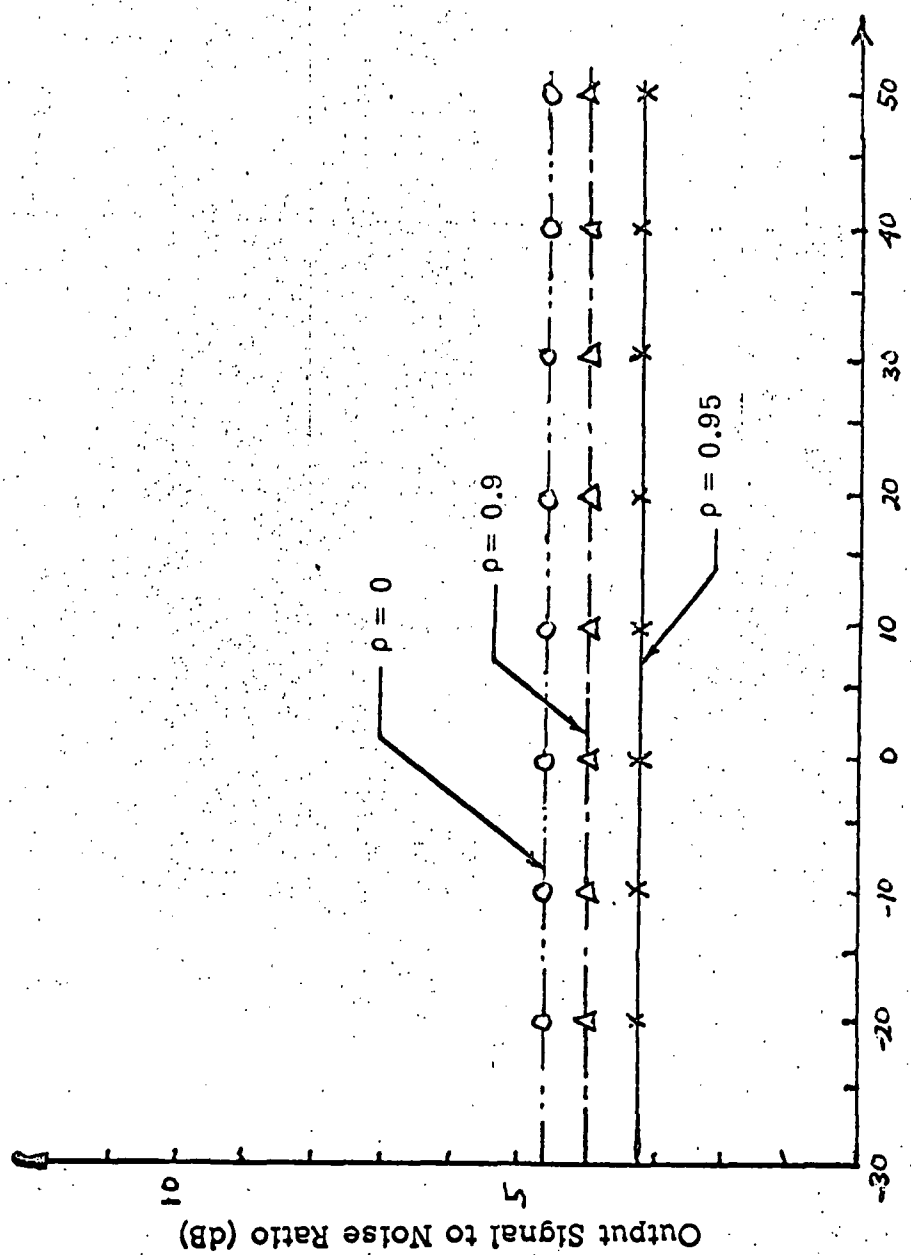

Fig. 6 Performance Curves of the Optimum Decoder for One Past Sample Observation

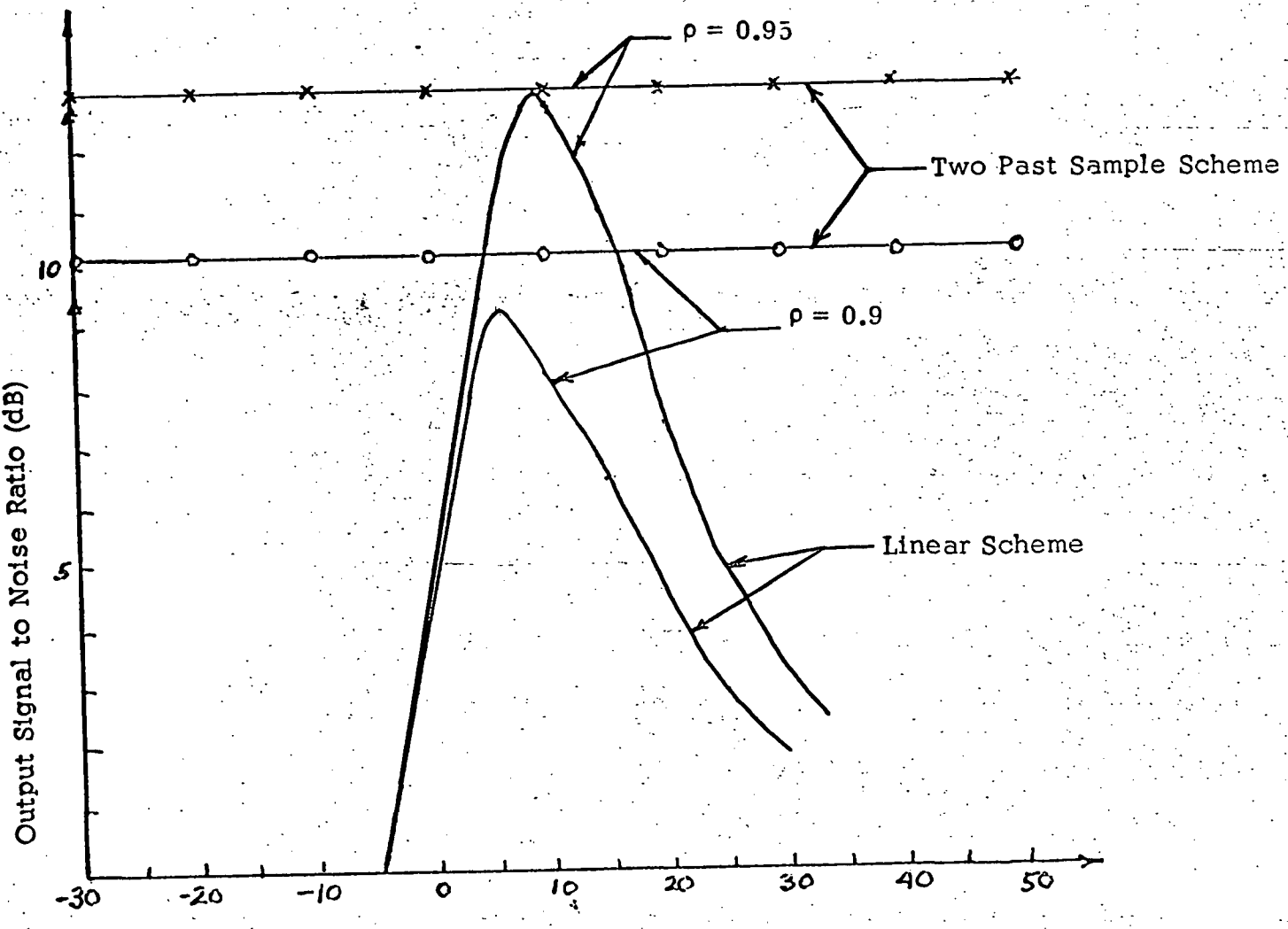

Fig. 7 Approximated Two Past Sample Scheme Compared to the Linear Delta Modulator

Curve A: Rate Distortion Bound for $\rho = 0.95$

B: Rate Distortion Bound for $\rho = 0.9$

C: Performance of the Two Past Sample Case for $\rho = 0.95$

D: Performance of the Two Past Sample Case for $\rho = 0.9$

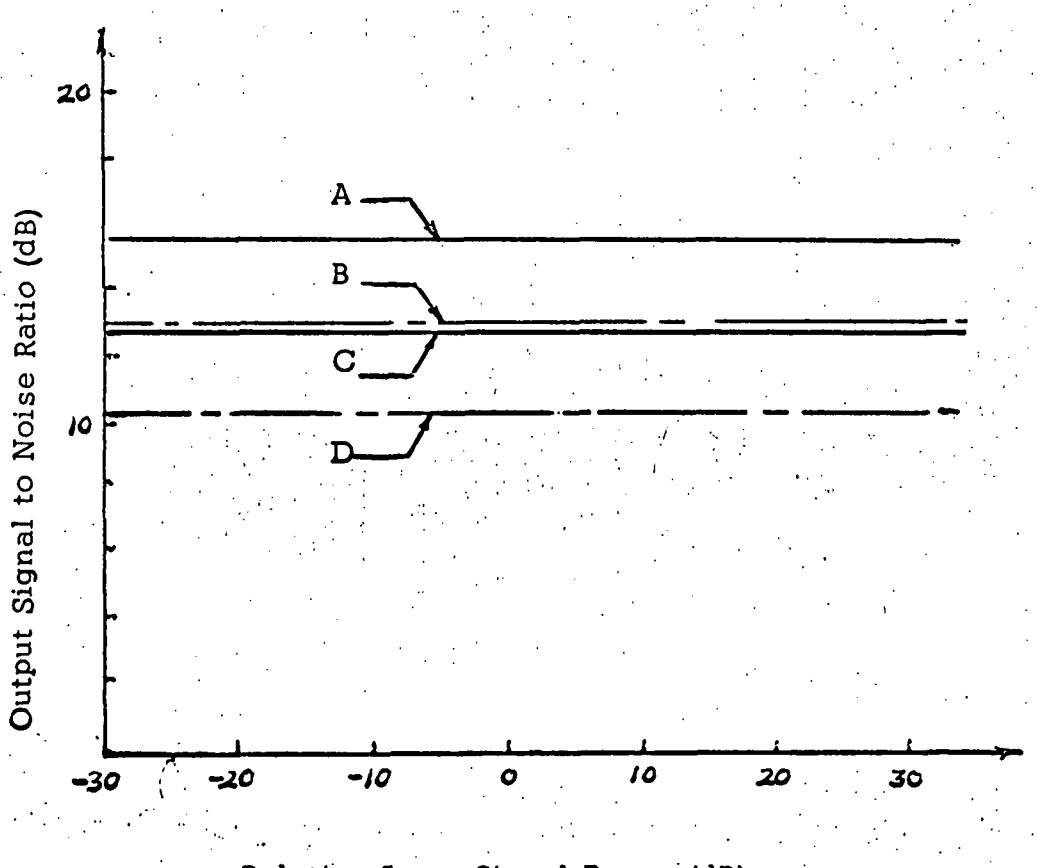

Fig. 8 Comparison of the Performance of the Two Past Sample Case to the Rate Distortion Bound

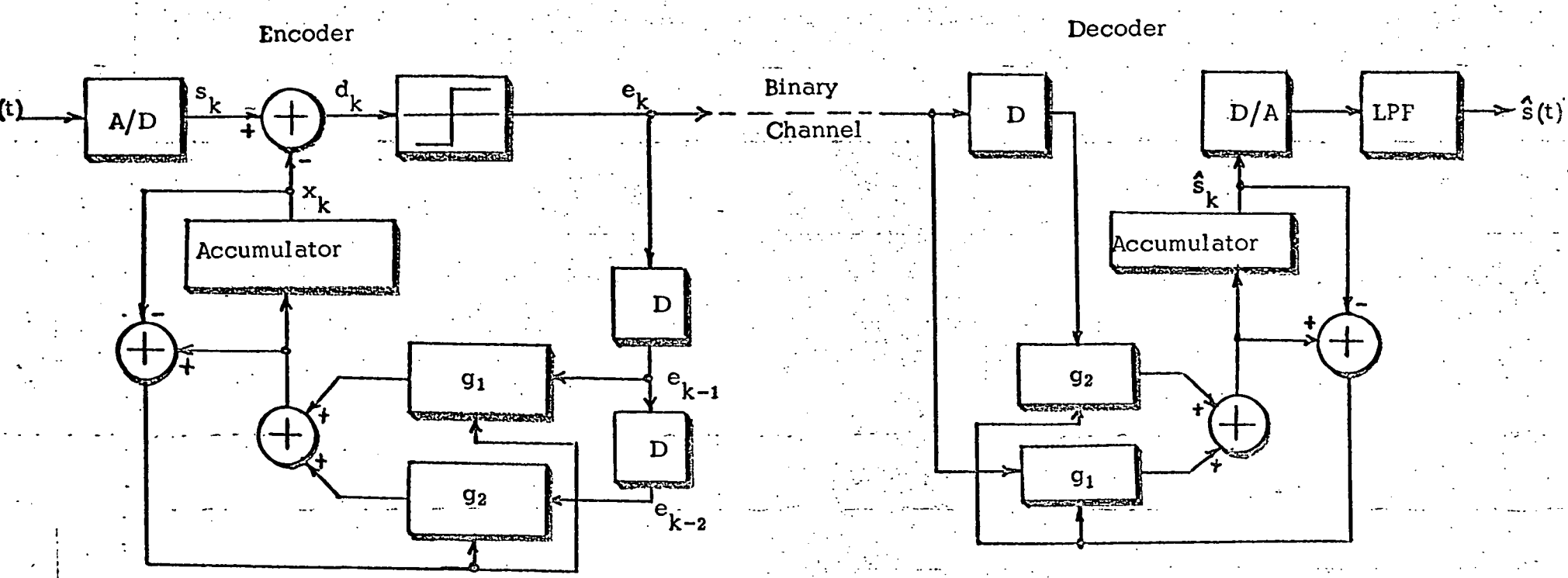

Fig. 9 Implemented Structure of the Variable Step Size Robust Delta Modulator-Demodulator

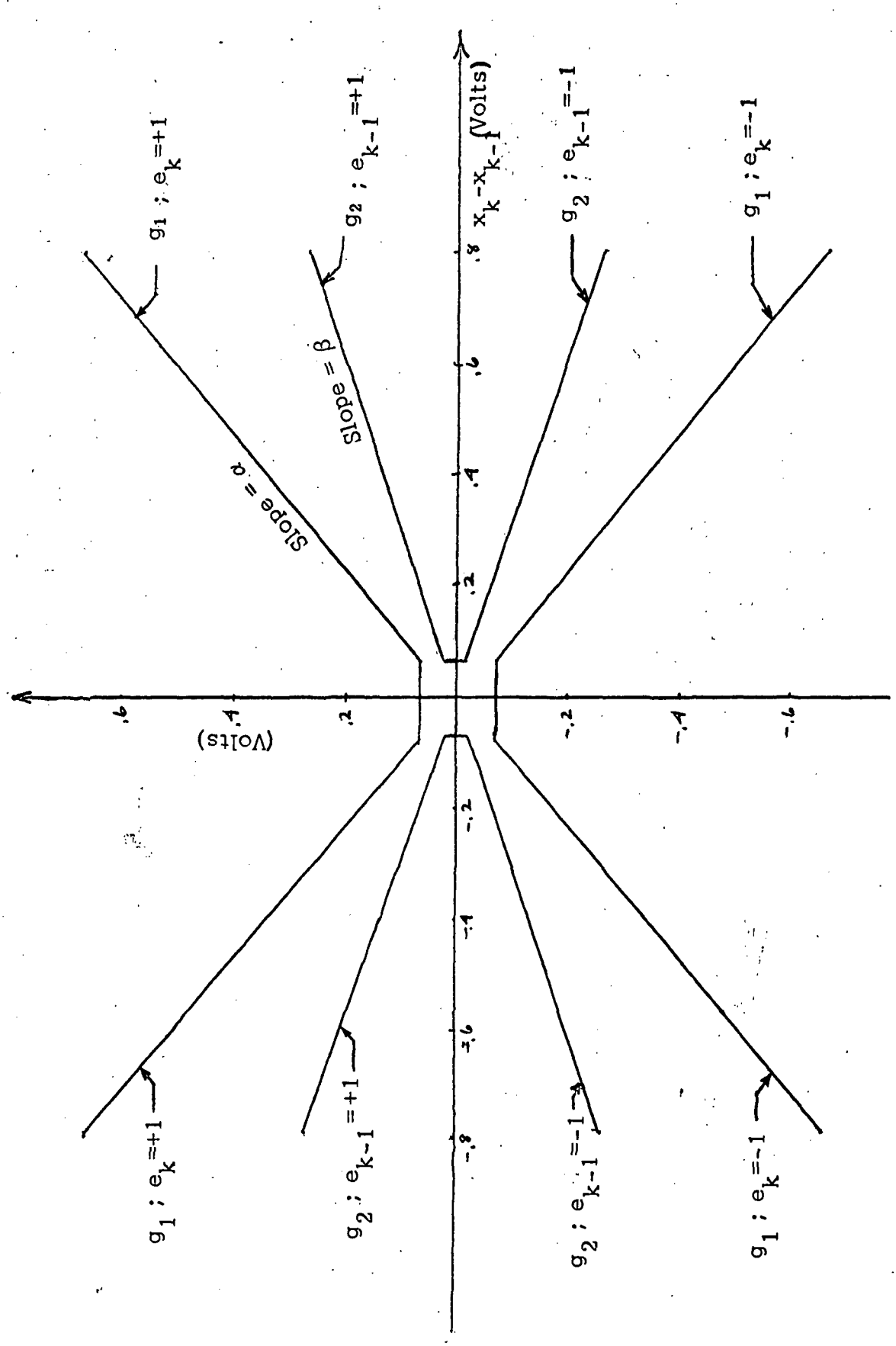

Fig. 10 Function Generators for the Two Past Sample Scheme

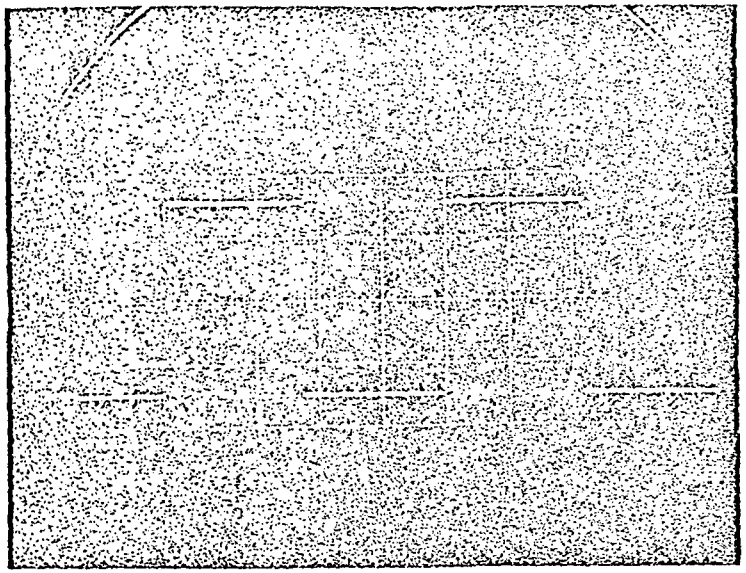

500 Hz Square Wave Input

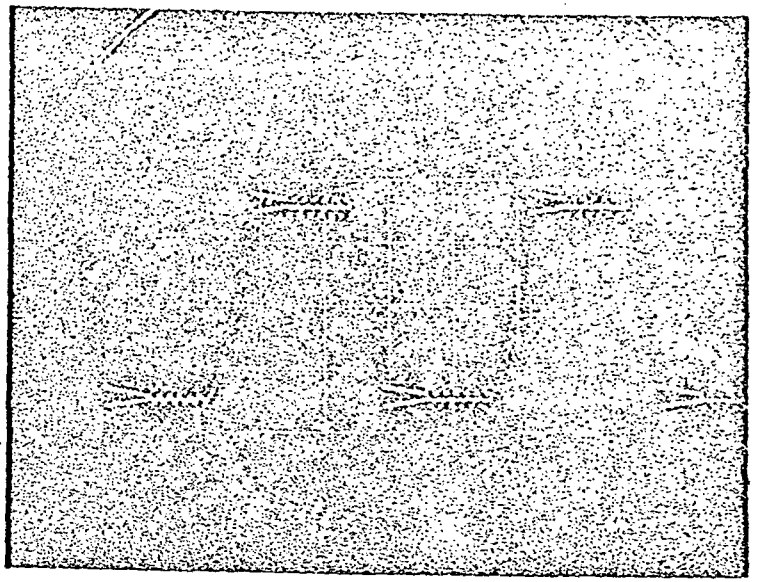

Adaptive Delta Modulator α=1, β=0

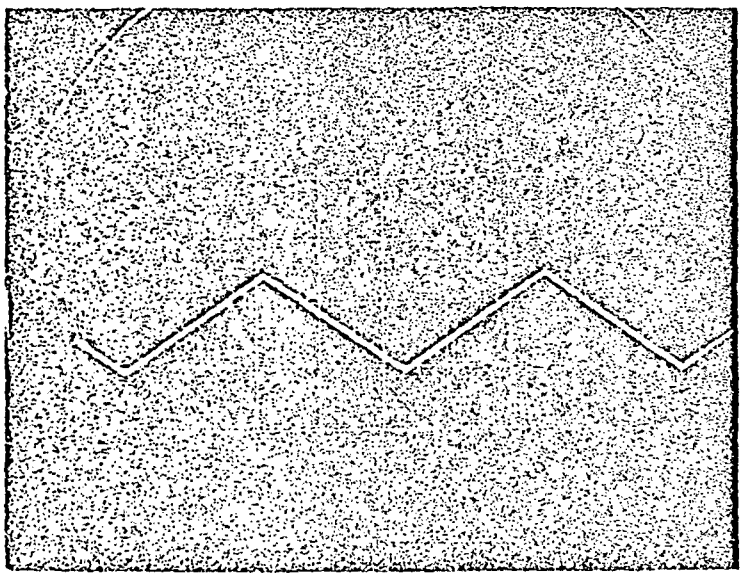

Linear Delta Modulator

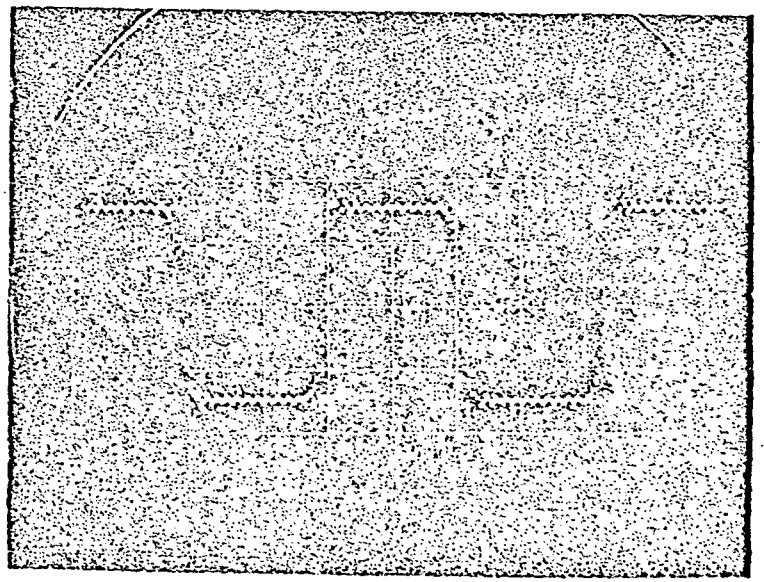

Adaptive Delta Modulator α=1, β=0.5

Fig 11 Responses to a 500 Hz Square Wave

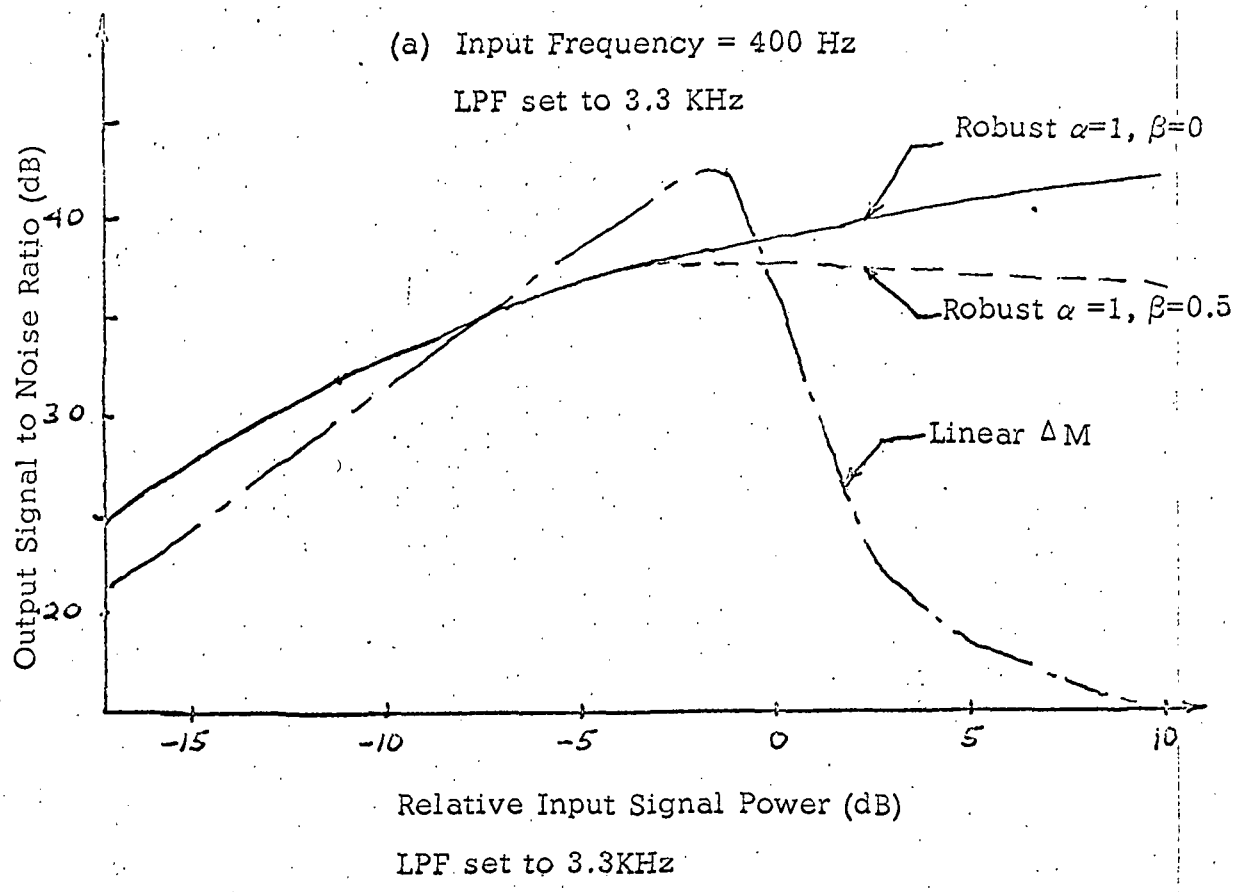

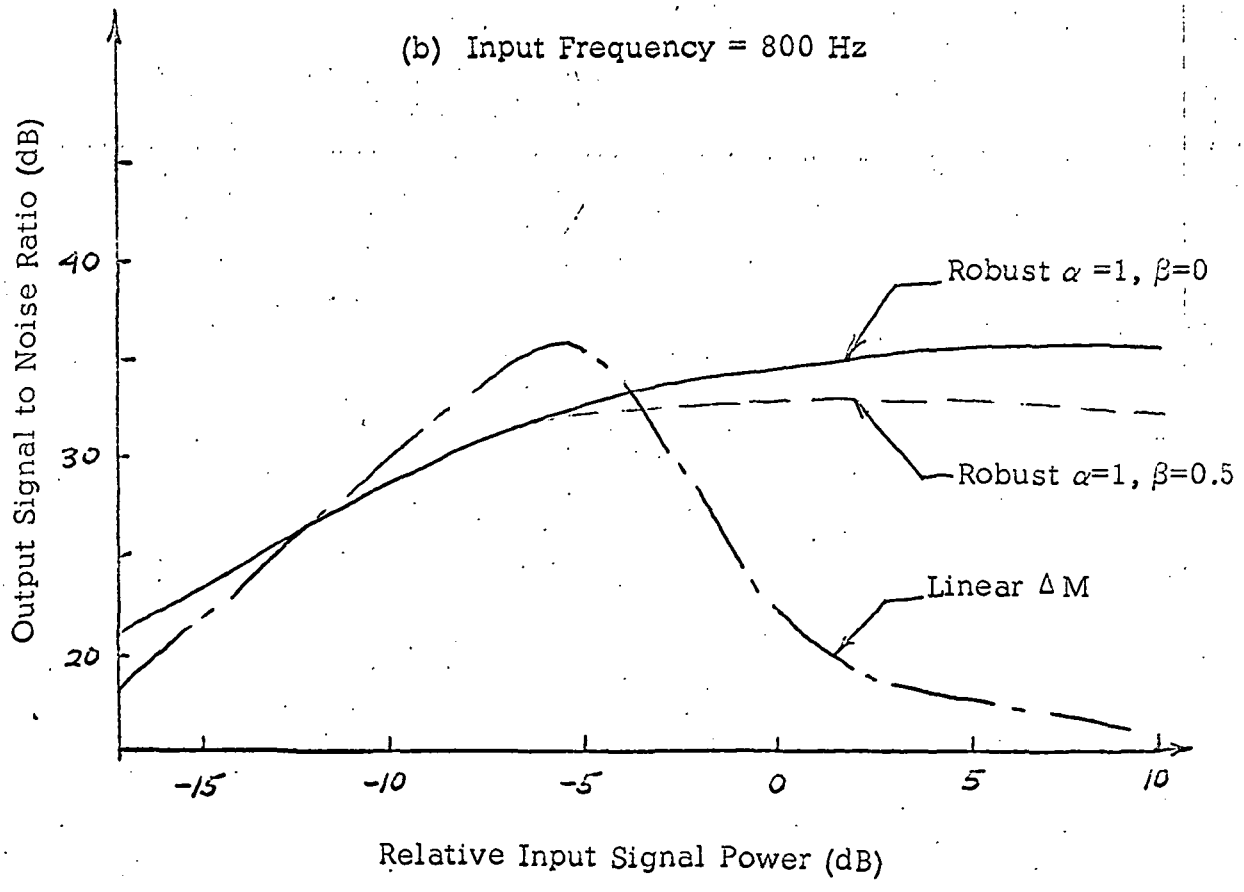

Fig 12 Response of the Variable Step Size Robust Delta Modulator Compared to the Linear Delta Modulator

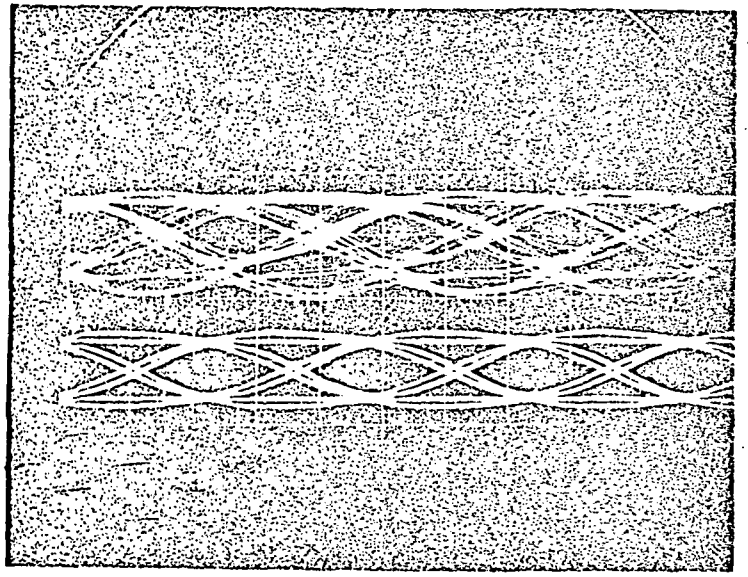

Fig 13a Eye Pattern of the Linear Delta Modulator

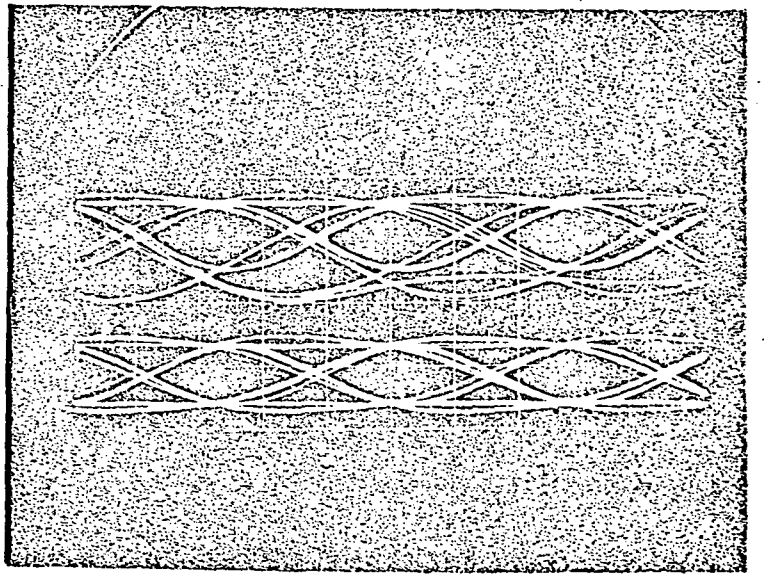

Fig 13b Eye Pattern of the Adaptive Delta Modulator (α=1, β=0.5)

Appendix I

Derivation of Equation (6)

$$P(s_k \mid e_k x_k) = \frac{\partial}{\partial s_k} F(s_k \mid e_k, x_k)$$

where

$F(x) \triangleq$ cummulative function of a random variable x

$$F(s_k \mid e_k x_k) = P_r(\underline{s_k} < s_k \mid e_k, x_k)$$

Since $\underline{s_k} > x_k$ for $e_k = +1$

and $\underline{s_k} < x_k$ for $e_k = -1$

we have

$$F(s_k \mid x_k, e_k = +1) = P_r(\underline{s_k} < s_k \mid s_k > x_k)$$

$$= \frac{P_r(\underline{s_k} < s_k,\ s_k > x_k)}{P_r(\underline{s_k} > x_k)} = \frac{\int_{x_k}^{s_k} P(s_k')\, ds_k'}{q'\left(\frac{x_k}{\sigma_{s_k}}\right)}$$

$$P(s_k \mid x_k, e_k = +1) = \frac{\partial}{\partial s_k} F(s_k \mid x_k, e_k = +1) = \frac{P(s_k)}{q'\left(\frac{x_k}{\sigma_{s_k}}\right)} \quad \text{for } s_k > x_k$$

and

$$P(s_k \mid x_k, e_k = +1) = 0 \qquad \text{for } s_k < x_k$$

Similarly for $e_k = -1$

$$P(s_k \mid x_k, e_k = -1) = \begin{cases} \dfrac{P(s_k)}{q\left(\frac{x_k}{\sigma_{s_k}}\right)} & \text{for } s_k < x_k \\ 0 & \text{for } s_k > x_k \end{cases}$$

Appendix II

Proof of Equation (8)

When $e_{k-1}, e_k = +1$

$$P(s_k \mid x_{k-1}^k, e_{k-1} = -1, e_k = +1) = \frac{\partial}{\partial s_k} F(s_k \mid x_{k-1}^k, e_{k-1} = -1, e_k = +1)$$

$$= \begin{cases} \dfrac{\int_{-\infty}^{x_{k-1}} P(s_{k-1}, s_k)\, ds_{k-1}}{\int_{-\infty}^{x_{k-1}} \int_{x_k}^{\infty} P(s_{k-1}, s_k)\, d(s_{k-1}, s_k)} & \text{for } s_k > x_k \\ 0 & \text{for } s_k < x_k \end{cases}$$

Thus,

$$r_k = E(s_k \mid x_{k-1}^k, e_{k-1} = -1, e_k = +1) = \frac{\int_{-\infty}^{x_{k-1}} \int_{x_k}^{\infty} s_k\, P(s_{k-1}, s_k) d(s_{k-1}, s_k)}{\int_{-\infty}^{x_{k-1}} \int_{x_k}^{\infty} P(s_{k-1}, s_k)\, d(s_{k-1}, s_k)} = \frac{N(-1,+}{D(-1,+}$$

Since $s_k = \rho_{k-1}\, s_{k-1} + \lambda_{k-1}$,

$$P(s_k \mid s_{k-1}) = \frac{1}{\sqrt{2\pi}\,\sigma_{s_{k-1}}} \exp\left[-\frac{(s_k - \rho_{k-1}\, s_{k-1})^2}{2\,\sigma^2_{\lambda_{k-1}}} \right]$$

The denominator

$$D(-1, +1) = \int_{-\infty}^{x_{k-1}} \int_{x_k}^{\infty} P(s_k \mid s_{k-1})\, P(s_{k-1})\, ds_{k-1}\, ds_k$$

Let

$$t_{k-1} \triangleq \frac{s_k - \rho_{k-1}\, s_{k-1}}{\sigma_{\lambda_{k-1}}}; \qquad z_{k-1} \triangleq \frac{x_k - \rho_{k-1}\, s_{k-1}}{\sigma_{\lambda_{k-1}}}$$

Then

$$D(-1, +1) = \int_{-\infty}^{x_{k-1}} \left[\int_{z_{k-1}}^{\infty} \frac{1}{\sqrt{2\pi}} \exp\left(-\tfrac{1}{2}\, t_{k-1}^2 \right) dt_{k-1} \right] P(s_{k-1})\, ds_{k-1}$$

$$= \int_{-\infty}^{x_{k-1}} q'(z_{k-1})\, P(s_{k-1})\, ds_{k-1}$$

The numerator

$$N(-1,+1) = \int_{-\infty}^{x_{k-1}} \int_{x_k}^{\infty} s_k \, P(s_{k-1}, s_k) \, d(s_{k-1}, s_k) = \int_{-\infty}^{x_{k-1}} \left[\int_{x_k}^{\infty} s_k P(s_k | s_{k-1}) ds_{k-1} \right] P(s_{k-1}) \, ds_{k-1}$$

Since the integral

$$\int_{x_k}^{\infty} s_k \, P(s_k | s_{k-1}) ds_{k-1} = \int_{z_{k-1}}^{\infty} \frac{1}{\sqrt{2\pi}} (\rho_{k-1} s_{k-1} + \sigma_{\lambda_{k-1}} t_{k-1}) \exp\left(-\frac{t_{k-1}^2}{2}\right) dt_{k-1}$$

$$= \rho_{k-1} \, s_{k-1} \, q'(z_{k-1}) + \frac{\sigma_{\lambda_{k-1}}}{\sqrt{2\pi}} \exp\left(\frac{z_{k-1}^2}{2}\right)$$

Hence,

$$N(-1,+1) = \int_{-\infty}^{x_{k-1}} \left[\rho_{k-1} s_{k-1} q'(z_{k-1}) + \frac{\sigma_{\lambda_{k-1}}}{\sqrt{2\pi}} \exp\left(-\tfrac{1}{2} z_{k-1}^2\right) \right] P(s_{k-1}) \, ds_{k-1}$$

Therefore,

$$r_k(-1,+1) = \frac{N(-1,+1)}{D(-1,+1)} = \text{Eq. (8-a)}$$

Similarly, Eq. (8-b), (8-c) and (8-d) can be proved by following the same procedures.

Appendix III

Derivation of Equation (10)

With the approximation shown in Eq. (9), when $e_{k-1} = -1$, $e_k = +1$, the denominator of Eq. (8-a) becomes:

if $\dfrac{x_k}{\rho_{k-1}} < x_{k-1}$

Then $D_k(-1, +1) = \int_{-\infty}^{\frac{x_k}{\rho_{k-1}}} \frac{1}{2} e^{-az^2_{k-1}} P(s_{k-1})\, ds_{k-1} + \int_{\frac{x_k}{\rho_{k-1}}}^{x_{k-1}} (1-\frac{1}{2}e^{-az^2_{k-1}})P(s_{k-1})ds_{k-1}$

$= q(\alpha_{k-1}) - q(\frac{\gamma_{k-1}}{\rho_{k-1}}) + \int_{-\infty}^{\frac{x_k}{\rho_{k-1}}} e^{-az^2_{k-1}} P(s_{k-1})ds_{k-1} - \frac{1}{2}\int_{-\infty}^{x_{k-1}} e^{-az^2_{k-1}} P(s_{k-1})ds_{k-1}$

where $\alpha_{k-1} \triangleq \dfrac{x_{k-1}}{\sigma_{s_{k-1}}}$; $\gamma_{k-1} \triangleq \dfrac{x_k}{\sigma_{s_{k-1}}}$; $z_{k-1} \triangleq \dfrac{x_k - \rho_{k-1} s_{k-1}}{\sigma_{\lambda_{k-1}}}$

Define $\beta_{k-1} = (2a\,\rho_{k-1}\sigma^2_{s_{k-1}} + \sigma^2_{\lambda_{k-1}})^{\frac{1}{2}}$; $y'_k = \dfrac{x_{k-1} - \frac{2a\rho_{k-1}x_k\sigma^2_{s_{k-1}}}{\beta^2_{k-1}}}{\frac{\sigma_{s_{k-1}}\sigma_{\lambda_{k-1}}}{\beta_{k-1}}}$

$$r_k = \frac{\frac{x_k}{\rho_{k-1}} - \frac{2a\rho_{k-1}x_k\sigma^2_{s_{k-1}}}{\beta^2_{k-1}}}{\frac{\sigma_{s_{k-1}}\sigma_{\lambda_{k-1}}}{\beta_{k-1}}} \quad ; \quad y''_k = y'_k \,(a = \tfrac{1}{2})$$

After completing the square of the exponents and integrating, the denominator becomes

$$D_k(-1,+1) = q(\alpha_{k-1}) - q(\frac{\gamma_{k-1}}{\rho_{k-1}}) + \frac{\sigma_{\lambda_{k-1}}}{\beta_{k-1}} \left[q(r_k) - \tfrac{1}{2} q(y'_k) \right] \exp\left[\frac{ax^2_k}{\beta^2_{k-1}}\right] \qquad \text{(A-1)}$$

if $\dfrac{x_k}{\rho_{k-1}} > x_{k-1}$

$$D_k(-1, +1) = \int_{-\infty}^{x_{k-1}} \tfrac{1}{2} \exp(-az^2_{k-1})\, P(s_{k-1})\, ds_{k-1}$$

$$= \frac{\sigma_{\lambda_{k-1}}}{2\beta_{k-1}} q(y_k) \exp\left[-\frac{ax^2_k}{\beta^2_{k-1}}\right] \qquad \text{(A-2)}$$

The numerator of Eq. (8-a) becomes the following:

if $\frac{x_k}{\rho_{k-1}} < x_{k-1}$

$$N_k(-1,+1) = \int_{-\infty}^{\frac{x_k}{\rho_{k-1}}} \left[\tfrac{1}{2}\rho_{k-1}s_{k-1}\exp(-az_{k-1}^2) + \frac{\sigma\lambda_{k-1}}{\sqrt{2\pi}}\exp(-\tfrac{1}{2}z_{k-1}^2) \right] P(s_{k-1})\, ds_{k-1}$$

$$+ \int_{x_k/\rho_{k-1}}^{x_{k-1}} \left[\rho_{k-1}s_{k-1}\left\{ 1-\tfrac{1}{2}\exp(-az_{k-1}^2) \right\} + \frac{\sigma\lambda_{k-1}}{\sqrt{2\pi}}\exp(-\tfrac{1}{2}z_{k-1}^2) \right] P(s_{k-1})ds_{k-1}$$

$$= \frac{\sigma^2_{\lambda_{k-1}}}{\sqrt{2\pi}\beta'_{k-1}} q(y_k'')\exp(-\frac{x_k^2}{2\beta'^2_{k-1}}) - \frac{\rho_{k-1}\sigma s_{k-1}}{\sqrt{2\pi}}\exp(-\frac{\alpha^2_{k-1}}{2}) + \frac{\rho_{k-1}\sigma s_{k-1}}{\sqrt{2\pi}}\exp(-\frac{\gamma^2_{k-1}}{2\rho^2_{k-1}})$$

$$+ \rho_{k-1}\int_{-\infty}^{\frac{x_k}{\rho_{k-1}}} s_{k-1}\exp(-az_{k-1}^2)\, P(s_{k-1})ds_{k-1} - \frac{\rho_{k-1}}{2}\int_{-\infty}^{x_{k-1}} s_{k-1}\exp(-az_{k-1}^2)P(s_{k-1})\, ds_{k-1}$$

where $\beta'_{k-1} = \beta_{k-1}(a=\frac{1}{2})$

Since the integral

$$\int_{-\infty}^{x_{k-1}} s_{k-1}\exp(-az_{k-1}^2)\, P(s_{k-1})\, ds_{k-1}$$

$$= \left[\frac{2a\rho_{k-1}x_k\sigma^2 s_{k-1}\sigma\lambda_{k-1}}{\beta^3_{k-1}} q(y'_k) - \frac{\sigma^2_{\lambda_{k-1}}\sigma s_{k-1}}{\sqrt{2\pi}\beta^2_{k-1}}\exp(-\tfrac{1}{2}y_k^2) \right]\exp(-\frac{ax_k^2}{\beta^2_{k-1}})$$

$$N_k(-1,+1) = \frac{\rho_{k-1}\sigma s_{k-1}}{\sqrt{2\pi}}\exp(-\frac{\gamma^2_{k-1}}{2\rho^2_{k-1}}) - \frac{\rho_{k-1}\sigma s_{k-1}}{\sqrt{2\pi}}\exp(-\frac{\alpha^2_{k-1}}{2}) + \frac{\sigma^2_{\lambda_{k-1}}}{\sqrt{2\pi}\beta'_{k-1}} q(y_k'')\exp(-\frac{x_k^2}{2\beta'^2_{k-1}})$$

$$+ \rho_{k-1}\left[\frac{2ax_k\rho_{k-1}\sigma s^2_{k-1}\sigma\lambda_{k-1}}{\beta^3_{k-1}} \left\{ q(r_k) - \tfrac{1}{2}q(y'_k) \right\} - \frac{\sigma^2_{\lambda_{k-1}}\sigma s_{k-1}}{\sqrt{2\pi}\beta^2_{k-1}} \left\{ \exp(-\tfrac{1}{2}r_k^2) \right.\right.$$

$$\left.\left. - \tfrac{1}{2}\exp(-\tfrac{1}{2}y'^2_k) \right\} \right]\exp(-\frac{ax_k^2}{\beta^2_{k-1}}) \qquad \text{(A-3)}$$

if $\frac{x_k}{\rho_{k-1}} > x_{k-1}$

$$N_k(-1,+1) = \int_{-\infty}^{x_{k-1}} \left[\tfrac{1}{2}\rho_{k-1} s_{k-1} \exp(-az_{k-1}^2) + \frac{\sigma_{\lambda_{k-1}}}{\sqrt{2\pi}} \exp(-\tfrac{1}{2}z_{k-1}^2) \right] P(s_{k-1}) ds_{k-1}$$

$$= \frac{\sigma_{\lambda_{k-1}}^2}{\sqrt{2\pi}\beta'_{k-1}} q(y''_k) \exp\left(-\frac{x_k^2}{2\beta'^2_{k-1}}\right) + \frac{\rho_{k-1}}{2} \left[\frac{2a\rho_{k-1} x_k \sigma_{\lambda_{k-1}} \sigma^2 s_{k-1}}{\beta^3_{k-1}} q(y'_k) \right.$$

$$\left. \frac{\sigma^2_{\lambda_{k-1}} \sigma_{s_{k-1}}}{\sqrt{2\pi}\beta^2_{k-1}} \exp\left(-\tfrac{1}{2}y_k^2\right) \right] \exp\left(-\frac{ax_k^2}{\beta^2_{k-1}}\right) \qquad \text{(A-4)}$$

Therefore, for $\frac{x_k}{\rho_{k-1}} < x_{k-1}$

$$r_k(-1,+1) = \frac{N_k(-1,+1)}{D_k(-1,+1)} = \frac{\text{Eq. (A-3)}}{\text{Eq. (A-1)}} \qquad \text{(A-5)}$$

for $\frac{x_k}{\rho_{k-1}} > x_{k-1}$

$$r_k(-1,+1) = \frac{N_k(-1,+1)}{D_k(-1,+1)} = \frac{\text{Eq. (A-4)}}{\text{Eq. (A-2)}} \qquad \text{(A-6)}$$

if $a=\frac{1}{2}$, and $\sigma^2_{s_{k-1}} >> \sigma^2_{\lambda_{k-1}}$

$y'_k = y''_k \approx y_k$, $\beta_{k-1} = \beta'_{k-1} \approx \rho_{k-1}\sigma_{s_{k-1}}$, $y'_k \approx r_k$

$\alpha_{k-1} \approx \frac{\gamma_{k-1}}{\rho_{k-1}}$

Therefore Eq. (A-5) and Eq. (A-6) reduce to eq. (10-a). By following the same procedure Eq. (10-b), Eq. (10-c) and Eq. (10-d) can be derived.

Appendix IV

The rate distortion function of the first order Gaussian Markov Source with the autocorrelation function

$$R(k) = \rho^{|k|}\,\sigma_s^2$$

has been found to be (6)

$$R(D) = \tfrac{1}{2}\log_2 \frac{(1-\rho^2)\,\sigma_s^2}{D} \text{ (bits/sample)} \qquad 0 < D < \theta_1$$

where $\theta_1 = \frac{1-\rho}{1+\rho}\,\sigma_s^2$

Since the ΔM system can transmit at most one bit per sample,

$$1 = \tfrac{1}{2}\log_2 \frac{(1-\rho^2)\,\sigma_s^2}{D} \qquad 0 < D < \frac{1-\rho}{1+\rho}\,\sigma_s^2$$

where

$$D = \frac{(1-\rho^2)\,\sigma_s^2}{4}$$

Therefore,

$$\text{SNR} = 10 \log \frac{\sigma_s^2}{D} = 10 \log \frac{4}{1-\rho^2}$$

Hence,

for $\rho = 0.95$ SNR = 16dB

for $\rho = 0.9$ SNR = 13.2dB

Acknowledgment

Further details on this subject matter can be found in the work completed by C. L. Song, Ph.D. dissertation, Department of Electrical Engineering, Polytechnic Institute of Brooklyn, Brooklyn, New York, June 1971. The authors are grateful to Mr. T. Cassa and Mr. S. Altmann for their assistance in the implementation.

References

1. O'Neal, J. B. Jr., "Delta Modulation Quantizing Noise Analytical and Computer Simulation Results for Gaussian and Television Input Signals." Bell Sys. Tech. J., January, 1966.

2. Tomozawa, A., and Kaneko, H., "Companded Delta Modulation for Telephone Transmission," IEEE Trans. on Communication Technology, Vol. Com-16, No. 1, pp. 149-157, February 1968.

3. Brolin, S. J., and Brown, James M., "Companded Delta Modulation for Telephony," IEEE Trans. on Communication Technology Vol. Com-16, No. 1, pp. 157-162, February 1968.

4. Abate, J. E., "Linear and Adaptive Delta Modulation," Proceedings of the IEEE Vol. 55, No. 33, pp. 298-308, March 1967.

5. Winkler, M. R., "High Information Delta Modulation," IEEE International Conv. Rec., pt. 1, pp. 285-290, 1965.

6. Gish, H., "Optimum Quantization of Random Sequences," Ph.D. dissertation, Harvard Unviersity, Cambridge, Mass., 1967.